Measurements of secondary particles produced from thick targets bombarded by heavy ions

Tadahiro KUROSAWA[1)], Takashi NAKAMURA[1)], Noriaki NAKAO[2)]
Tokushi SHIBATA[3)], Yoshitomo UWAMINO[4)] , Akifumi FUKUMURA[5)]

[1)]Cyclotron and Radioisotope Center, Tohoku University
Aoba, Aramaki, Aoba-ku, Sendai, 980-8578, Japan
kurosawa@cyric.tohoku.ac.jp
[2)]High Energy Accelerator Research Organization, Tanashi Branch
Midori-cho 3-2-1,Tanashi,Tokyo,188-8501, Japan
[3)] High Energy Accelerator Research Organization
Oho-cho 1, Tsukuba, Ibaraki, 305-0801, Japan
[4)]Institute of Physical and Chemical Research
Hirosawa 2-1,Wako, Saitama 351-0198, Japan
[5)]National Institute of Radiological Sciences
Anagawa 4-9-1, Inageku, Chiba-shi, 263-8555, Japan

We measured angular and energy distributions of neutrons, protons, deuterons and tritons produced by 100 MeV/nucleon He ions stopping in thick carbon, aluminum, copper and lead targets using the HIMAC (Heavy Ion Medical Accelerator in Chiba) of NIRS (National Institute of Radiological Sciences), Japan by using the time-of-flight method coupled with the ΔE-E counter system. The experimental spectra were compared with the calculation using the LCS code and the calculated spectra are generally in rather good agreement with the measured spectra of these four secondary particles.

1. INTRODUCTION

With the increasing use of high energy (higher than 100MeV/nucleon) heavy ions (heavier than He ion) in various fields, the energy-angle distribution of neutrons produced from a thick target which fully stops heavy ions becomes very important as the source-term data of shielding design of the accelerator facility. Although only one paper has ever been published on thick target neutron yield (TTY) for 177MeV/nucleon He ions [1], Heilbronn et al. [2] and our group [3, 4] have recently performed the experiments on TTY for 155MeV/nucleon He ions [2] and for 100, 180 MeV/nucleon He and 100, 180, 400MeV/nucleon C ions [3] , and for 100, 180, 400MeV/nucleon Ne ions [4]. In this work we present the angular - energy distributions of neutrons, protons, deuterons and tritons produced from thick carbon, aluminum, copper and lead targets bombarded by 100 MeV/nucleon helium ion. The charged particle spectra from thick targets are not so important in physical meaning due to the energy loss in the target depending on the target thickness, but these results will be useful as benchmark experimental data to investigate the accuracy of the particle-transport calculation code. Here, the measured spectra are compared with those calculated with the LAHET Code System, LCS [5] as a benchmark test.

2. EXPERIMENTAL PROCEDURE

The energy of neutrons, protons, deuterons and tritons produced in the target was measured by the time-of-flight (TOF) method. A thin NE102A plastic scintillator (3cm diam. by 0.05cm thick) was placed just behind the end window of the beam line as a beam pick-up scintillator. The output pulses of this scintillator were used as start signals of the TOF measurement, and also to count the absolute number of projectiles incident on the target. A target was set on the beam line 10 cm behind the beam pick-up scintillator. The beam spot size incident on the target was about 1.5 cm diameter and the beam height was 1.25m above the concrete floor of the experimental area. The NE213 liquid scintillator (12.7cm diam. by 12.7cm thick), which was designed to expand the dynamic range of output pulses for high energy neutron measurements[6], was used for neutron detector (E counter), and the NE102A plastic scintillator (15 cm by 15cm square and 0.5cm thick) for the ΔE counter was placed in front of the E counter to discriminate charged particles from noncharged particles, neutrons and photons. Three sets of E and ΔE counters were used for simultaneous angular distribution measurements at three different angles. The detectors were located 2 m at large angles to 5 m at small angles away from the target to provide better energy resolutions in the forward directions where there are larger yields of high energy neutrons. In order to minimize

neutrons in scattering, no local shielding was used near the detectors. By interposing an iron shadow bar of 15cm by 15cm square and 60cm thickness between the target and detector, the background neutron components from room scattering were measured particularly at large angle. Target thicknesses were selected to stop the incident particles completely. Target materials are C (1.77g/cm^3), Al (2.7g/cm^3), Cu (8.93g/cm^3) and Pb (11.34g/cm^3) and each target has a shape of 10cm by 10cm square. The C, Al, Cu and Pb targets are 5.0, 4.0, 1.5 and 1.5 cm thick, respectively.

3. DATA ANALYSIS

3.1 Neutrons

As the ΔE counter does not scintillate by neutrons and gamma rays, the neutron and gamma ray events could be selected from the charged particle events, by using two-dimensional ΔE-E graphical plots shown in Fig. 1 (a). After this discrimination, the neutron and the gamma ray events were clearly separated by using two-dimensional graphical plots of total-slow pulse height components of the E counter as shown in Fig. 1 (b). In this discrimination, the pulse shapes from high energy neutron events in which recoil protons escape from the E counter are close to those from gamma-ray events, and these events were eliminated from the neutron events. After each experimental run, each E counter was calibrated with a ^{60}Co gamma-ray source, and the Compton edge in the gamma-ray spectrum was used as the bias point of 1.25MeVee (electron equivalent) which corresponded to 3 MeV neutron energy. After obtaining the TOF spectrum of neutrons, the data were converted into the energy spectrum of neutrons. For this conversion, the detection efficiency of the NE213 E counter is essential. The experimental data of the detection efficiency for this scintillator has been published by Nakao et al.[6], but there is no data for neutrons of energy higher than 135MeV. Therefore, the neutron detection efficiency was calculated with the Monte Carlo code by Cecil et al.[7] for all energy range. Corresponding to the elimination of high energy neutron events as described above, the recoil proton events escaped from the E counter were also excluded from these calculated efficiencies.

3.2 Charged particles

To separate proton, deuteron and triton events, three kinds of two dimensional graphical plots were used. Two dimensional ΔE-E graphical plots in Fig. 1(a) were first used to identify different Z number particles, but this plots could not identify different mass number particles. From Fig. 1(a) only Z=1 particles were selected, and only a small fraction of Z=2 particles can be seen in Fig. 1(a) because the incident alpha particles fully stopped in a thick target. The two dimensional plots of TOF-E pulse height distributions for Z=1 particles are shown in Fig. 2(a). In Fig. 2(a), different mass particles of protons (m=1) deuterons (m=2) and tritons (m=3) are clearly separated, but the pulse heights of high energy particles escaped from the E counter intersect between those of different mass particles. This intersection was resolved in the following way. It is well known that slow components from the NE213 scintillator increase with increasing the specific energy loss (dE/dx) for a given type of charged particle. The charged particles escaped from the detector, which have the longer stopping range than the detector size, give small dE/dx values compared with the charged particles stopped in the detector and then slow components of the light outputs from escaped particles approach to the pulse heights of gamma rays. These results are shown in the two dimensional total-slow pulse height plots. The proton, deuteron and alpha particles have three separate lines in the order of dE/dx values of these three particles and the charged particles escaped from the detector are in the uppermost line independent to the particle mass. We first selected proton events by setting the region of interest (ROI) in Fig. 2(a) which included the events of escaped deuterons and tritons, and then eliminated the latter events by identifying the escaped particle events, as shown in Fig. 2(b). This procedure was repeated for deuterons and tritons in this order. We finally obtained the TOF spectra for protons, deuterons and tritons separately. The TOF spectra were then converted to the energy spectra by approximating 100% detection efficiency of the NE213 detector.

4. MONTE CALRO SIMULATIONS

These experimental results were compared with the calculations as a benchmark test. The secondary particle spectra were calculated by using the LAHET Monte Carlo Code System, LCS[5]. The LCS calculations were performed for 100MeV/nucleon He incidence on stopping-length C, Al, Cu and Pb targets to investigate the calculational accuracy. The majority of the LAHET parameters was set to their default settings. The target dimension was fixed to be the same size as used in the experiment. The target was set at the center of the vacuum sphere and a total number of 200,000 He particles were injected normally to the target in the central circular surface of 0.5 cm diameter which simulated the actual beam geometry. The angular flux of particles of neutrons, protons, deuterons and tritons emerged from the target were stored at each angle corresponding to the

experimental results.

5. RESULTS AND DISCUSSIONS

5.1 Neutron spectra

Fig. 3 shows the experimental and calculated neutron spectra. Neutron spectra measured in the forward direction have a plateau peak at high energy end which corresponds to about 60 to 70 % of the projectile energy per nucleon. This peak is mainly due to high energy neutron components produced in the forward direction by a break-up process and becomes more prominent for lighter target, since the momentum transfer from projectile to target nuclei are higher for lighter nucleus than for heavier nucleus. The high energy neutrons in the forward direction spread up to the energy which is about the twice as much as the incident particle energy per nucleon. The calculated spectra shown in Fig. 3 generally give rather good agreement with the experimental results in absolute values. Precisely speaking, the following three tendencies can be seen between experiments and calculations. In the calculation, a broad high energy peak in the forward direction appears more distinctly around incident particle energy per nucleon, compared with more flattened high energy peak in the experiment. This discrepancy also reveals that the LCS calculation gives the underestimation of the neutron spectra in the intermediate energy region of 5 to 50 MeV. The calculated spectra at angles larger than 30 degree are harder than the measured spectra, which means that the LCS calculation gives the underestimation of evaporation neutrons and the overestimation of pre-equilibrium neutrons extended to higher energy region.

5.2 Proton spectra

The experimental proton spectra are shown in Fig 4. The lower energy limit in the measured spectra was estimated to be 27MeV considering the proton energy absorption through the air between the target and the detector (500cm), the ΔE counter (0.5cm thick plastic of $CH_{1.104}$ and the density of $1.032 g/cm^3$) and the aluminum cover (0.5mm thick) of the E counter. These energy absorption was calculated for proton, deuteron and triton using the SPAR code [8], and the lower energy limits of proton, deuteron and triton which are reachable to the E counter are then estimated to be 27.0, 36.6 and 43.7MeV. Although proton spectra are similar to neutron spectra in shapes and absolute values at forward angles, proton yields rapidly decrease with increasing angles. At large angles, low energy proton components are dominant which can easily be absorbed by the thick target itself. Compared with measured and calculated proton spectra, the LCS calculation for proton spectra gives rather good agreement with the experiment in the forward direction.

5.3 Deuteron spectra

The experimental deuteron spectra are shown in Fig. 5. At 90 degree, the deuterons emitted from the target could not be detected because of its strong forwardness. Measured spectra in the forward direction have a broad peak around 140MeV and yields decrease drastically with increasing angles. For C target, the calculated and experimental results agree well at 0, 7.5, 15 and 60 degrees. At 30 degree, the calculated spectrum is larger than the measured one. As a general tendency, the agreement between calculated and measured deuteron spectra is surprisingly good.

5.4 Triton spectra

The experimental triton spectra are shown in Fig. 6. Triton could not be detected at 60 and 90 degrees because of much stronger forwardness than deuteron. Measured spectra in the forward direction have a broad peak around 200MeV and yields decrease drastically with increasing angles. In the triton spectra, the LCS calculation gives good agreement with the experiment in the forward direction, especially for heavier target.

6. CONCLUSION

We measured angular and energy distributions of neutrons, protons, deuterons and tritons produced by 100 MeV/nucleon helium ions stopping in carbon, aluminum, copper and lead targets. The experimental spectra were compared with the calculation using the LCS code and the calculated spectra are generally in rather good agreement with the measured spectra for these four secondary particles. These experimental results were found to be useful as the benchmark data for investigating the accuracy of high energy particle transport calculation code.

Acknowledgments

We gratefully acknowledge the support and assistance of the accelerator operation staff of HIMAC. This work was supported in part by the Research Project with Heavy Ions at NIRS-HIMAC.

References

[1] Cecil, R. A. et al., Phys. Rev., **C21**, 2471(1980)
[2] Heilbronn, L. et al., to be published in Nucl. Sci. Eng. May issue, 1999
[3] Kurosawa, T. et al., to be published in Nucl. Sci. Eng. May issue, 1999
[4] Kurosawa, T. et al., to be published in J. Nucl. Sci. Technol., January issue, 1999.
[5] Prael, R.E. and Lichtenstein, H., LA-UR-89-3014, Los Alamos National Laboratory (1989)
[6] Nakao, N. et al., Nucl. Instr. Meth. Phys. Res. **A362** 454(1995)
[7] Cecil, R. A. et al., Nucl. Instr. and Meth. **161** 439(1979)
[8] Armstrong T.W. and Chandler K.C., Oak Ridge National Laboratory Report ORNL-4869 (1973)

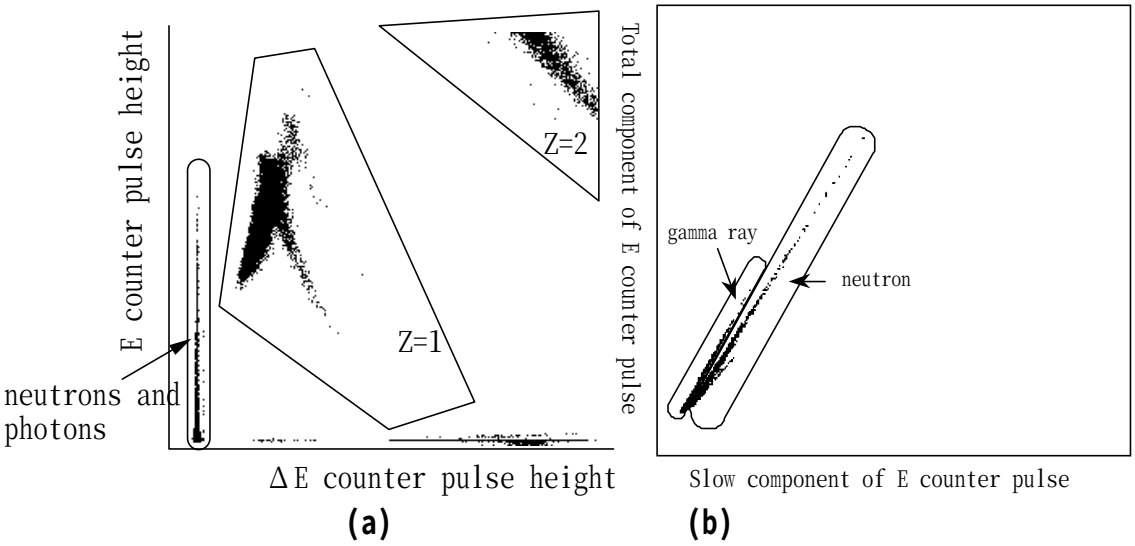

Fig. 1 (a) Two dimensional plot of E and ΔE counter pulse heights and (b) total and slow pulse heights.

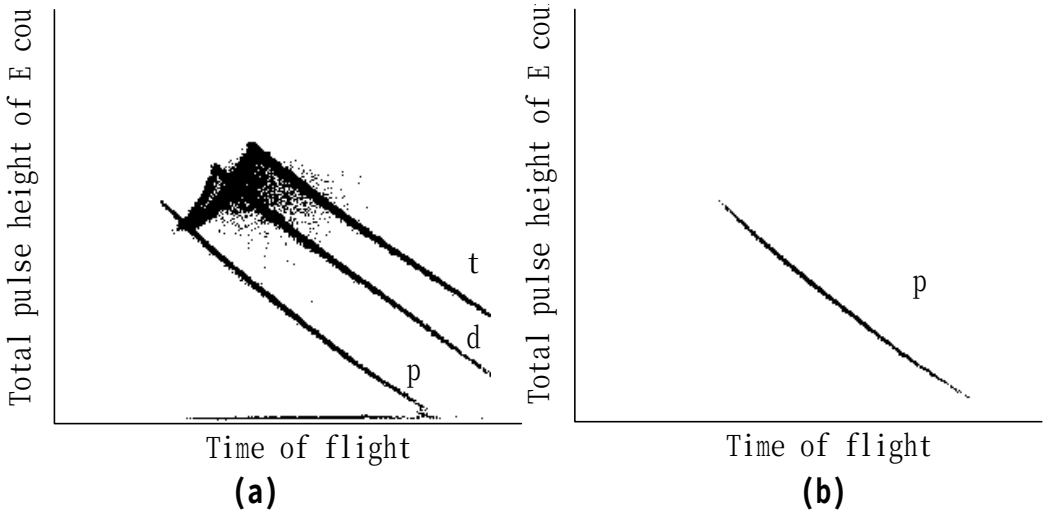

Fig. 2 (a) Two dimensional plot of TOF- E counter pulse height for Z=1 events selected from two dimensional plot of E and ΔE counter pulse heights and (b) that of only proton events.

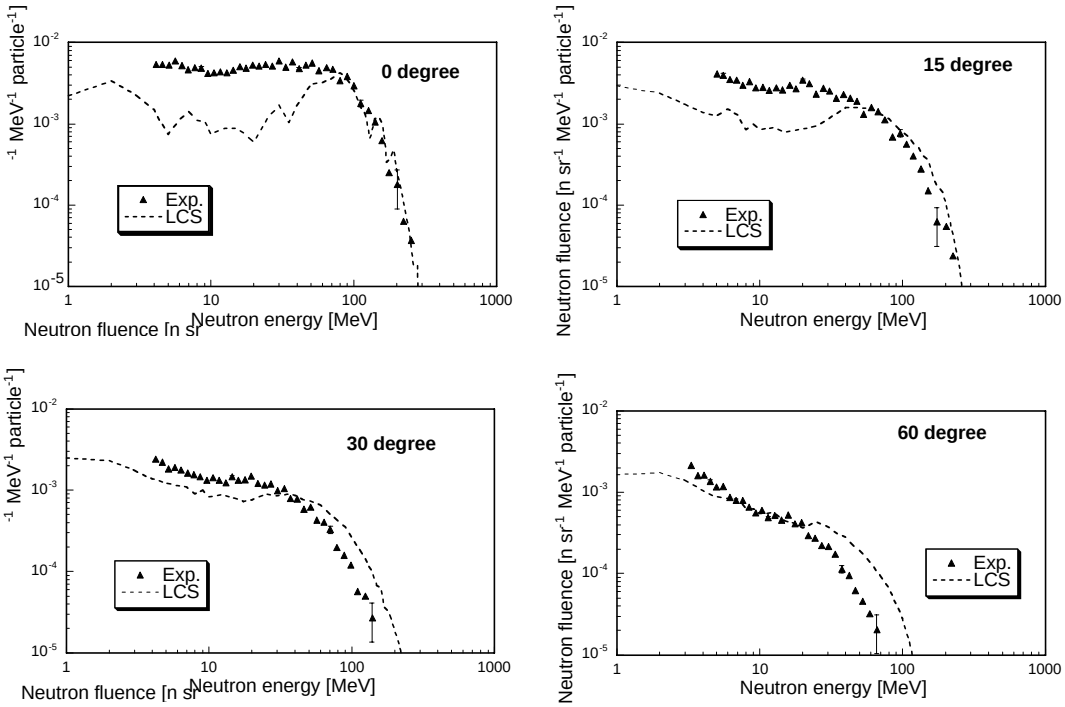

Fig. 3 Comparison of measured and calculated neutron spectra from carbon target.

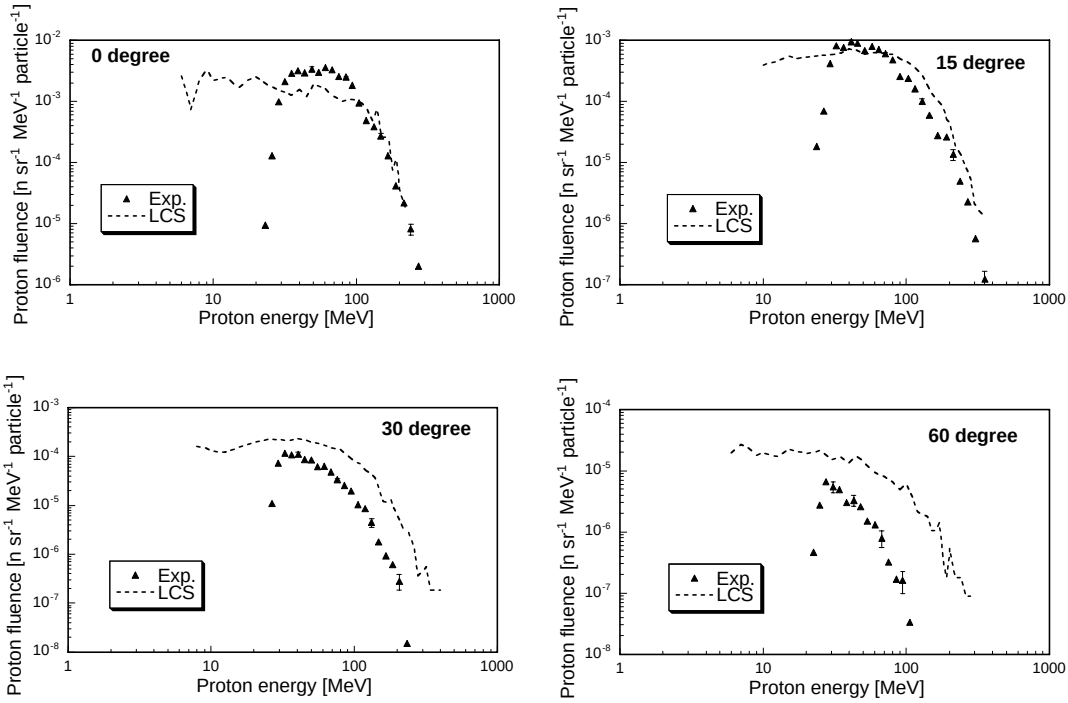

Fig. 4 Comparison of measured and calculated proton spectra from carbon target.

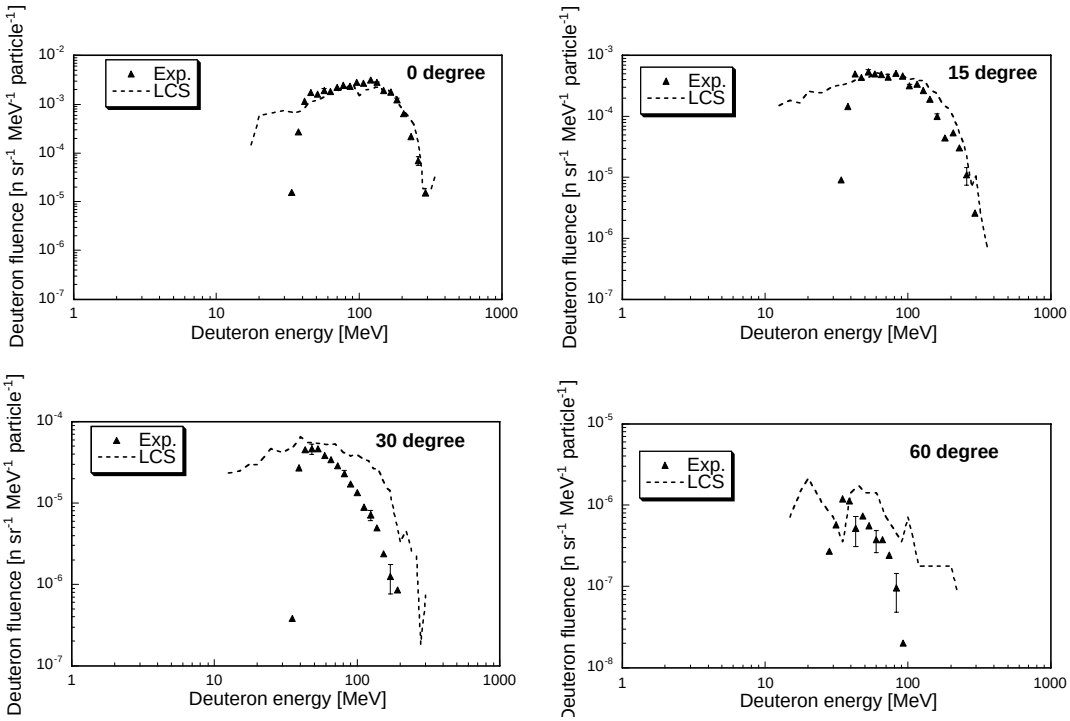

Fig. 5 Comparison of measured and calculated deuteron spectra from carbon target.

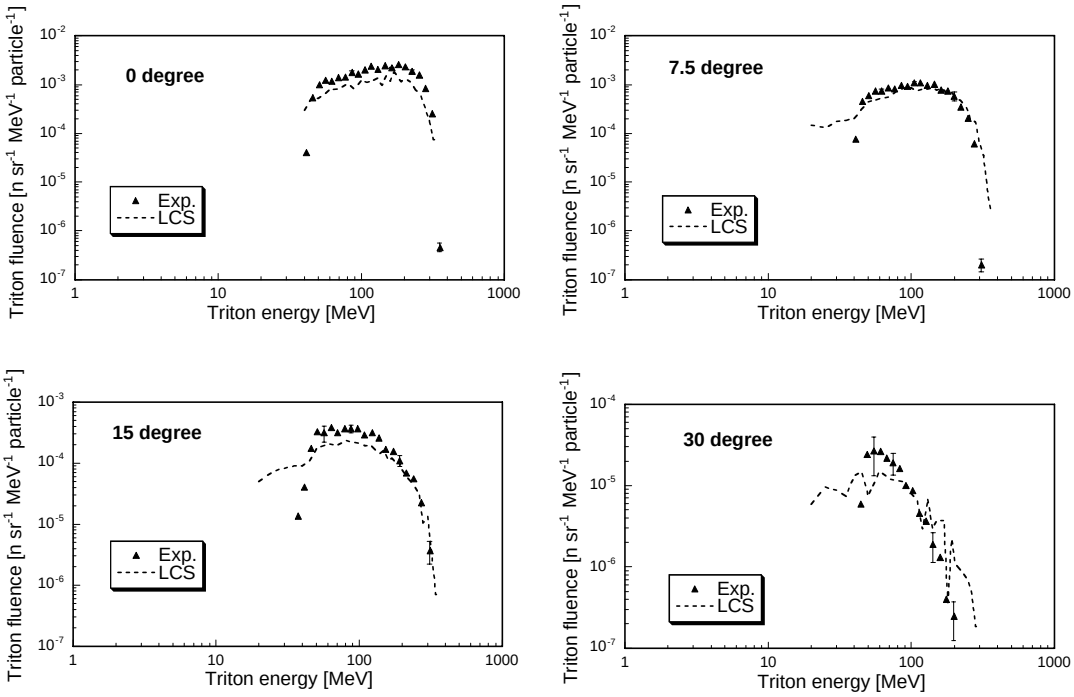

Fig. 6 Comparison of measured and calculated triton spectra from carbon target.